molecules

MDPI

Article

Aziridination Reactivity of a Manganese(II) Complex with a Bulky Chelating Bis(Alkoxide) Ligand

Sudheer S. Kurup [1], Natalie M. Woodland [2], Richard L. Lord [2,*] and Stanislav Groysman [1,*]

[1] Department of Chemistry, Wayne State University, 5101 Cass Ave., Detroit, MI 48202, USA
[2] Department of Chemistry, Grand Valley State University, 1 Campus Drive, Allendale, MI 49401, USA
* Correspondence: lordri@gvsu.edu (R.L.L.); groysman@wayne.edu (S.G.)

Abstract: Treatment of $Mn(N(SiMe_3)_2)_2(THF)_2$ with bulky chelating bis(alkoxide) ligand [1,1′:4′,1′′-terphenyl]-2,2′′-diylbis(diphenylmethanol) (H_2[O-terphenyl-O]^{Ph}) formed a seesaw manganese(II) complex Mn[O-terphenyl-O]$^{Ph}(THF)_2$, characterized by structural, spectroscopic, magnetic, and analytical methods. The reactivity of Mn[O-terphenyl-O]$^{Ph}(THF)_2$ with various nitrene precursors was investigated. No reaction was observed between Mn[O-terphenyl-O]$^{Ph}(THF)_2$ and aryl azides. In contrast, the treatment of Mn[O-terphenyl-O]$^{Ph}(THF)_2$ with iminoiodinane PhINTs (Ts = *p*-toluenesulfonyl) was consistent with the formation of a metal-nitrene complex. In the presence of styrene, the reaction led to the formation of aziridine. Combining varying ratios of styrene and PhINTs in different solvents with 10 mol% of Mn[O-terphenyl-O]$^{Ph}(THF)_2$ at room temperature produced 2-phenylaziridine in up to a 79% yield. Exploration of the reactivity of Mn[O-terphenyl-O]$^{Ph}(THF)_2$ with various olefins revealed (1) moderate aziridination yields for *p*-substituted styrenes, irrespective of the electronic nature of the substituent; (2) moderate yield for 1,1′-disubstituted α-methylstyrene; (3) no aziridination for aliphatic α-olefins; (4) complex product mixtures for the β-substituted styrenes. DFT calculations suggest that iminoiodinane is oxidatively added upon binding to Mn, and the resulting formal imido intermediate has a high-spin Mn(III) center antiferromagnetically coupled to an imidyl radical. This imidyl radical reacts with styrene to form a sextet intermediate that readily reductively eliminates the formation of a sextet Mn(II) aziridine complex.

Keywords: alkoxides; aziridination; manganese; iminoiodinane

Citation: Kurup, S.S.; Woodland, N.M.; Lord, R.L.; Groysman, S. Aziridination Reactivity of a Manganese(II) Complex with a Bulky Chelating Bis(Alkoxide) Ligand. *Molecules* **2022**, *27*, 5751. https://doi.org/10.3390/molecules27185751

Academic Editors: Alexey M. Starosotnikov, Maxim A. Bastrakov and Igor L. Dalinger

Received: 15 August 2022
Accepted: 30 August 2022
Published: 6 September 2022

1. Introduction

The nitrogen equivalent of an epoxide, aziridine, is a three-membered heterocycle containing one nitrogen and two carbon atoms [1]. The combination of Baeyer strain and an electronegative element in a three-membered ring makes it susceptible to ring-opening reactions [2]. Because of the high reactivity of aziridines, they serve as intermediates in the total synthesis of natural products [3] and pharmaceuticals [4,5], exhibit diverse biological/biomedical functions [6,7], and have been used extensively in the synthesis of various heterocycles [8,9]. Different routes toward this useful functional group have been reported in the literature [1,2,10,11]. In the absence of transition metals, aziridine synthesis requires extreme conditions (high temperature and/or pressure) or the availability of highly reactive ylide-based precursors [12–14]. Generally, transition metal-catalyzed nitrene group transfer to olefins enables a more efficient route to aziridines, which also takes place under milder reaction conditions. Various nitrene transfer reagents, such as iminoiodinanes [15–18], organic azides [19], chloramine–T, and bromamine–T [20–22], can act as nitrene precursors to carry out this transformation. Catalysts based on noble metals, such as Ag [23–28], Rh [29–37], Ru [38–44], and Pd [45–47], were found to be reactive, with a wide variety of alkenes. Although these catalysts are often very efficient, the high cost and low availability of precious metals prompted interest in developing more sustainable catalysts based on earth-abundant and generally less toxic 3d metals [48,49]. Aziridination via nitrene transfer

using Mn and Fe porphyrins was reported early on by Breslow et al. [50]. The reactivity of porphyrinoid (porphyrin, corrole, and phthalocyanine), salen, and oxazoline ligands in aziridination has led to a growing interest among the scientific community in developing nitrogen-donor ligand-based aziridination catalysts with varying properties [48]. A significant number of Fe- and Co-based aziridination catalysts have been reported in the last decade, most of which are supported by nitrogen-donor ligands [51–66]. In recent years, a number of Fe-based aziridination catalysts supported by oxygen-donor [67,68] and carbon-donor [69–75] ligands have been reported as well. The stability and reactivity of formally high-oxidation state Fe and Co have been demonstrated to depend on ancillary ligand environments. While for weak-field nitrogen and oxygen ligand environments the reactions are generally postulated to proceed via highly reactive (and often not isolable) metal(III)-imidyl radical species, strong-field (carbene) ligation forms more stable Fe(IV) imides [76,77]. In contrast, the field of Mn-based aziridination catalysis has been less explored. Most reported Mn catalysts feature nitrogen-donor ligands [78–88], with the notable exception of the mixed nitrogen/oxygen donor set of salen ligands. The present work describes the aziridination reactivity of a Mn complex bearing an oxygen-ligand environment exclusively.

Group-transfer catalysts containing 3d transition metals coordinated with bulky bis(alkoxide) ligands are currently under investigation in our group [89,90]. Bis(alkoxide) ligand platforms provide weak-field ligand environments, leading to reactive nitrene- and carbene-transfer catalysts [91–96]. Using these systems, we demonstrated iron- and chromium-mediated nitrene transfer to form azoarenes and carbodiimides, respectively [91–94]. However, no aziridine formation was observed in the reactions of the chromium or iron systems with the combination of organoazides and styrene. To improve catalyst stability and performance, we recently synthesized a new chelating bis(alkoxide) ligand H_2[O-terphenyl-O]^{Ph} ([1,1′:4′,1″-terphenyl]-2,2″-diylbis(diphenylmethanol)) [97,98]. The resulting iron complex Fe[O-terphenyl-O]^{Ph}(THF)$_2$ (**1**, Scheme 1) demonstrated significantly more efficient catalytic performance in azoarene production [97]. The improved performance of the chelating bis(alkoxide) ligand [O-terphenyl-O]^{Ph} in catalysis prompted us to investigate the application of its complexes in olefin aziridination. Herein, we report the first example of an Mn-based aziridination catalyst featuring a low-coordinate, oxygen-only, bulky bis(alkoxide) ligand environment.

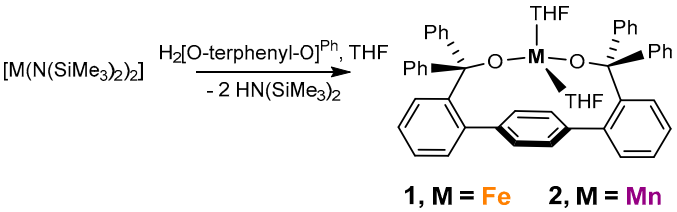

Scheme 1. Synthesis of Mn[O-terphenyl-O]^{Ph}(THF)$_2$ (**2**), along with the previously reported synthesis of iron analogue **1**.

2. Results and Discussion

*2.1. Reactivity of Fe[O-terphenyl-O]^{Ph}(THF)$_2$ (**1**) and Synthesis and Characterization of Mn[O-terphenyl-O]^{Ph}(THF)$_2$ (**2**)*

Complex **1** (Fe[O-terphenyl-O]^{Ph}(THF)$_2$) was prepared as previously described (Scheme 1) [97]. The attempted aziridination using the combination of an organoazide precursor (*p*-tolyl azide), styrene, and **1** (10 mol%) (room temperature) did not produce the desired 2-phenyl-1-(*p*-tolyl)aziridine product (Figure S14). However, replacing organoazide with the more reactive nitrene precursor iminoiodinane (PhINTs, Ts = *p*-toluenesulfonyl) produced 2-phenyl-1-tosylaziridine in 32% yield (Figure S15). In selected cases, Mn-based catalysts exhibited reactivity superior to their Fe-based counterparts [88]. We decided to prepare the Mn(II) analogue of **1** and explore its aziridination reactivity.

$Mn[O\text{-terphenyl-O}]^{Ph}(THF)_2$ (**2**) was synthesized by treating $Mn(N(SiMe_3)_2)_2(THF)_2$ with $H_2[O\text{-terphenyl-O}]^{Ph}$ in THF at room temperature (Scheme 1). The purple solution of the $Mn(N(SiMe_3)_2)_2(THF)_2$ precursor turned light yellow upon the addition of the ligand over a course of 8 hours. Recrystallization of the crude reaction product from CH_2Cl_2/THF mixture at −35 °C produced very pale yellow (nearly colorless) crystals of **2** in 74% yield. The product was characterized by solution magnetic measurements, X-ray crystallography, IR, and UV-vis spectroscopy, and elemental analysis. The solution state magnetic moment of **2** (measured in C_6D_6) was found to be 5.8 ± 0.2 μ_B (an average of two measurements), consistent with high-spin Mn(II) (Figures S3 and S4). ^{1}H NMR spectrum of the paramagnetic Mn(II) complex **2** demonstrated only two broad signals around 1.6 ppm and 3.8 ppm attributable to THF protons (Figures S1 and S2). The UV-vis spectrum in the 350–900 nm range was nearly featureless, as expected for high-spin Mn(II) (Figure S5).

The X-ray structure of **2** is presented in Figure 1 (crystal and refinement data are given in Table S4). As anticipated, $[O\text{-terphenyl-O}]^{Ph}$ binds to the metal in a chelating fashion. The geometry at the metal is a distorted seesaw, with a narrow angle between the THF ligands (91.3(2)°) and a wide angle between the alkoxide donors (150.3(2)°) (see Figure 1 for selected bond distances and angles). The seesaw geometry in **2** is similar to the previously reported iron counterpart **1** [97]. The inter-alkoxide angle (RO-Mn-OR, ~150°) in **2** is significantly wider than the corresponding angle in the related Mn(II) complex with two monodentate alkoxides ($Mn(OC^tBu_2Ph)_2(THF)_2$, ~130°) [99]. A similar difference in this angle was observed for the corresponding iron isologues $Fe[O\text{-terphenyl-O}]^{Ph}(THF)_2$ (**1**) and $Fe(OC^tBu_2Ph)_2(THF)_2$), [97,99,100] and likely resulted from the rigidity of the chelating para-terphenyl bis(alkoxide) framework. The distance between the central phenyl and Mn is 3.09 Å, suggesting no interaction between the phenyl ring and the metal center, as previously observed for the iron analogue [97]. In contrast, a considerably shorter distance between the metal and the central phenyl (2.49 Å) in the chromium analogue $Cr[O\text{-terphenyl-O}]^{Ph}(THF)_2$, was consistent with a weak covalent interaction between chromium and the central phenyl [98].

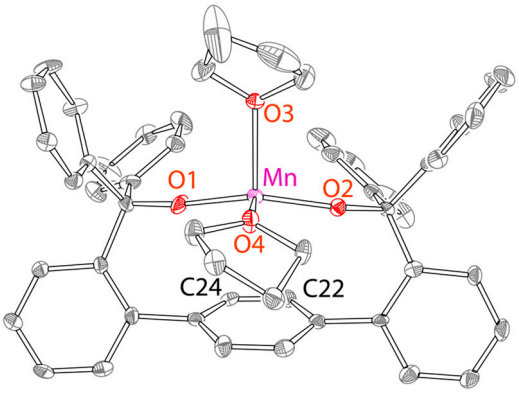

Figure 1. X-ray structure (50% probability) of $Mn[O\text{-terphenyl-O}]^{Ph}(THF)_2$ (**2**). Alternative conformations of one of the top THF ligands and one of the lateral phenyls, H atoms, and disordered solvent were omitted for clarity. Selected bond distances (Å) and angles (°): Mn-O1 1.888(5), Mn-O2 1.922(4), Mn-O3 2.205(4), Mn-O4 2.178(4), O1-Mn-O2 150.3(2), and O3-Mn-O4 91.23(2).

2.2. Reactivity of 2 in Aziridination

Following the synthesis and characterization of **2**, its reactivity in nitrene transfer was investigated. The reaction of **2** with representative organic aryl azides, including mesityl azide, *p*-tolyl azide, and tosyl azide in benzene, did not display any significant color change, even at elevated temperatures. No change in the ^{1}H NMR spectra of the reaction mixtures was observed, further suggesting a lack of reactivity. The reaction of **2** with organic azides in the presence of styrene or isocyanides similarly exhibited no change in the NMR spectrum of the reaction mixture. However, replacing the nitrene precursor with iminoiodinane (PhINTs, Ts = *p*-toluenesulfonyl) produced a rapid color change (colorless to brown). The

combination of PhINTs, styrene, and **2** (10 mol%, C_6D_6) for 24 h at room temperature led to the formation of the desired aziridine product, with 78% yield. The ^{1}H NMR spectrum of the reaction mixture (Figure S15) was relatively clean, exhibiting peaks attributable to the aziridine, styrene, and iodobenzene by-product. The control reaction of styrene (and other alkenes, see below) with PhINTs in the absence of a catalyst under similar reaction conditions formed trace amounts of $TsNH_2$; no formation of aziridines was observed.

To optimize catalyst performance, we carried out the aziridination of styrene at varying ratios of catalyst, PhINTs, and styrene (Table 1). In addition, we investigated the effects of different solvents on the reaction outcomes. All reactions were conducted at room temperature for 24 hours. Only small variations in product yields (74–78%) were observed for different ratios of styrene:PhINTs:catalyst in C_6D_6 (Table 1). These results are noteworthy, as a large excess of styrene is generally necessary in Mn-catalyzed aziridination reactions. The use of CD_2Cl_2 or CD_3CN as the reaction solvent produced similar yields at a 4:1 ratio of styrene:PhINTs (entries 1–3). However, in sharp contrast to C_6D_6, a significant decrease in the product yields was observed in these solvents when the styrene:PhINTs ratio was decreased to 1:1 (entries 6–8). It is feasible that a decrease in the product yields at a lower styrene:PhINTs ratio in polar solvents results from the increased solubility and therefore faster decomposition of reactive PhINTs in these solvents. As the reaction yield remained nearly optimal in benzene under less wasteful reaction conditions (reagent ratio of 1:1), it was used as a solvent in subsequent reactivity studies. Reducing catalyst loading to 5% (entry 5) led to a decline in the aziridine yield to 53%; a significant amount of undissolved PhINTs remained.

Table 1. Optimization of aziridination conditions.

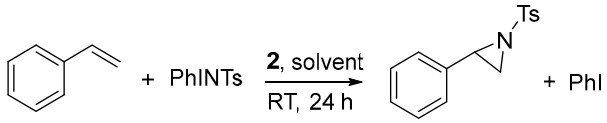

Entry	2 (mol%)	Solvent	PhINTs (equiv)	Styrene (equiv)	Yield (%)
1	10	C_6D_6	1	4	78
2	10	CD_2Cl_2	1	4	79
3	10	CD_3CN	1	4	70
4	10	C_6D_6	1	2	74
5	5	C_6D_6	1	2	53
6	10	C_6D_6	1	1	75
7	10	CD_2Cl_2	1	1	17
8	10	CD_3CN	1	1	43
9	10	C_6D_6	2	1	74
10	10	C_6D_6	1.5	1	75

Following the optimization of reaction conditions for styrene aziridination, the aziridination of additional olefins was investigated. All reactions were conducted at room temperature for 24 h using 10 mol% catalyst and a ratio of 1:1 PhINTs:styrene. The formation of the products was confirmed by ^{1}H NMR spectroscopy and GC-MS (see Supplementary Material). Several different variables in the olefin structure were investigated (Figure 2), including the electronic effect (*para* substitution) in styrene, the aromatic vs. aliphatic nature of mono-substituted olefins, and α- and β-disubstituted styrenes. The catalyst showed moderate reactivity with *p*-^{t}Bu, *p*-CN, and *p*-CF_3-substituted styrenes (52–54%); a slightly higher yield (62%) was obtained for electron-rich 4-methoxy styrene. In addition to the aziridine products, NMR spectra demonstrate the presence of an unreacted starting material (styrene) and the expected by-product iodobenzene. No additional products (e.g., $TsNH_2$ or C-H aminated products) were observed in significant quantities by ^{1}H NMR. However, the formation of these products in small quantities, or the formation of paramagnetic metal-based by-products, cannot be ruled out. The comparable reactivity of

electron-rich and electron-poor styrenes in Mn-catalyzed aziridination is consistent with previous reports [88]. No aziridination reactivity with non-aromatic olefins (methyl acrylate and 1-decene, Figures S21 and S22) was observed.

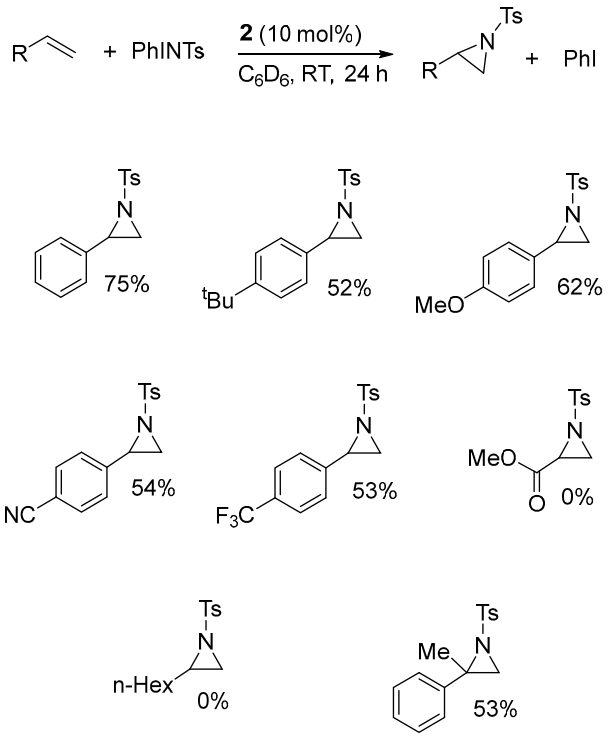

Figure 2. Aziridination of various olefins using **2**. The yields of the aziridine products were determined by ^{1}H NMR using internal standard (1,3,5-trimethylbenzene).

We also investigated the reactivity of α- and β-disubstituted styrenes. The reaction of α-methyl-styrene produced 1,1′-methylphenylaziridine relatively cleanly, with a moderate yield (53%). However, nitrene transfer onto β-disubstituted styrenes (*cis*/*trans* β-methyl-styrene and *cis*/*trans* stilbene) formed significantly more complex mixtures of products exhibiting broad resonances. Our attempts to isolate the organic products of these reactions were unsuccessful.

2.3. Spectroscopic and Computational Probing of the Reaction Mechanism

How does the formation of aziridine occur with **2** as a catalyst? Different mechanistic hypotheses for manganese-mediated aziridination with PhINTs were proposed, including via a Mn-N(Ts)IPh adduct or Mn=NTs imido [85,88]. We probed the nature of reactive intermediates by NMR spectroscopy and DFT calculations. PhINTs is insoluble in the reaction medium. Upon the combination of **2** with PhINTs in C_6D_6, its dissolution occurs. The ^{1}H NMR spectrum collected immediately after the dissolution of PhINTs (approximately 10–15 min) showed the formation of free PhI (iodobenzene, Figures S7–S9). Thus, the formation of PhI occurs concurrently with the formation of brown intermediates and dissolution of PhINTs, suggesting that Mn[O-terphenyl-O]^{Ph}-N(Ts)IPh is not a long-lived reaction intermediate. The addition of styrene after the formation of the brown intermediate shows aziridine formation, suggesting that the nitrene transfer to styrene does not take place via a Mn[O-terphenyl-O]^{Ph}-N(Ts)IPh intermediate. No $TsNH_2$ was observed by ^{1}H NMR after 15 min; formation of $TsNH_2$ was observed after approximately 20 h (Figures S10–S12). The UV-vis spectra of the mixtures of **2** with PhINTs, taken at different time intervals, were not informative (Figure S13). Because our multiple attempts to isolate reaction intermediates were not successful, we used DFT calculations to probe the nature of the reaction intermediates and the reaction mechanism.

Additional support for the short-lived iminoiodinane adduct comes from computations. DFT calculations of putative iminoiodinane adducts showed significant activation, as evidenced by the long N-I distances of 2.94 and 3.10 Å for the two isomers vs. 2.06 Å in free iminoiodinane (Figure S28). Mayer bond orders of only 0.08 and 0.05 confirm that the N-I bond is broken in both isomers. Moreover, the electronic structure of this species is nearly identical to that of the formal imido species (*vide infra*) formed after the loss of PhI. The reaction of **2** with two equivalents of PhINTs is unlikely due to steric constraints [86,98]. We hypothesize that the aziridination of styrene takes place via a Mn-imido intermediate.

Multiple geometries and possible oxidation/spin states were evaluated for the manganese imido species. The lowest energy quartet optimized structure is shown in Figure 3. This species has a short Mn-NTs bond length of 1.72 Å that is slightly longer than the known Mn-imido species of ~1.6 Å [101–103] and shorter Mn-O bond lengths of 1.75 and 1.78 Å than the crystal structure of the Mn(II) species (Figure 1). The spin isosurface shows that spin is mostly localized at Mn and N, with opposite spins on each atom in Figure 3; Mulliken spin densities are 3.5 for Mn, 0.0 for [O-terphenyl-O]^{Ph}, and −0.5 for NTs. This suggests that this quartet has an electronic structure between a formal high-spin Mn(IV)-imido and high-spin Mn(III)-imidyl, with antiferromagnetic coupling between the metal and ligand radical. This geometric and electronic structure is similar to the one reported for Mn with a triphenylamido amine ligand; thus, we consider it Mn(III)-imidyl going forward and computationally probe the radical mechanism previously proposed [88]. Analysis of the electronic structure of the iminoiodinane adduct showed Mulliken spins of 3.4 for Mn, 0.0 for [O-terphenyl-O]^{Ph}, and −0.4 for TsNIPh, and visualization of the spin density (see Supplementary Material) shows that it is localized on the N. Thus, that adduct is probably better interpreted as manganese imidyl with a van der Waals-bound PhI.

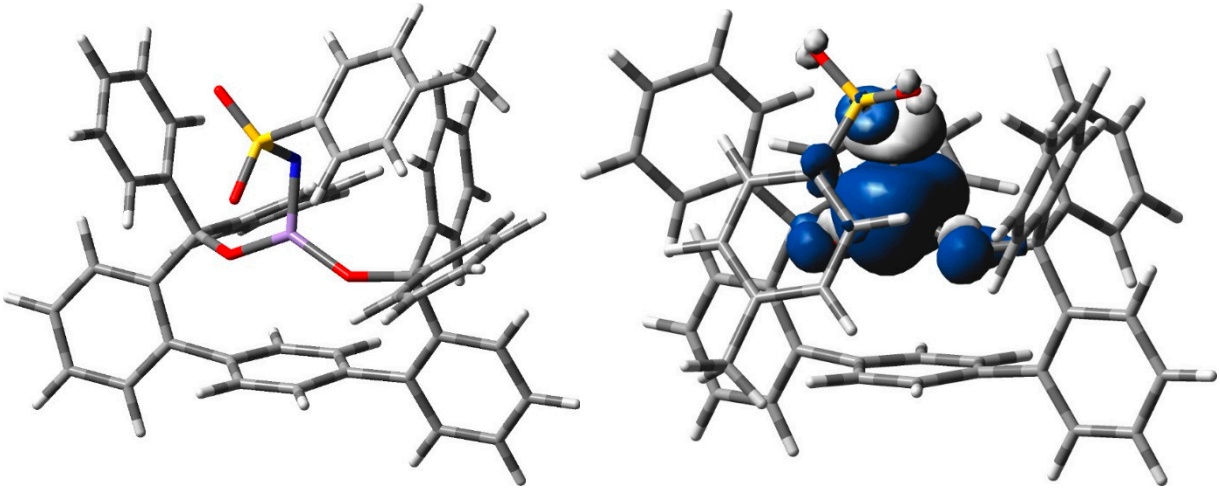

Figure 3. Optimized structure of the lowest energy quartet (**left**) and its spin density isosurface plotted using a cutoff value of 0.002 au (**right**). Blue and white surfaces correspond to excess alpha and beta spins, respectively.

Figure 4 summarizes the lowest energy structures along the reaction mechanism. Alternative regio and stereoisomers, and spin states are discussed in the Supporting Information. Starting with the bis-THF complex, the loss of both THF molecules is uphill by 13.2 kcal/mol. Binding of iminoiodinane to Mn[O-terphenyl-O]^{Ph} is exergonic by 28.3 kcal/mol and affords putative iminoiodinane adduct **A**, which we use as the reference point for this mechanism. As discussed above, **A** has a nearly identical electronic structure to Mn(III)-imidyl intermediate **B**, which is exergonic by 2.3 kcal/mol. **B** reacts with styrene on the quartet surface through a transition state that is 6.8 kcal/mol uphill in Gibbs free energy, and spin crossover occurs before the radical intermediate **C**, which is downhill in Gibbs energy by 12.4 kcal/mol relative to **B**. **C** has Mulliken spins of 4.0

for Mn, 0.0 for [O-terphenyl-O]^{Ph}, and 0.9 for NTsCH$_2$CHPh, the latter of which is mostly localized on CHPh (see Supplementary Material). The barrier between **C** and **D** is uphill by 4.9 kcal/mol, and **D** is exergonic by 7.0 kcal/mol. **D** has Mulliken spins of 4.8 for Mn, 0.1 for [O-terphenyl-O]^{Ph}, and 0.1 for aziridine. Thus, the high-spin Mn(III) intermediate **C** is well poised to reductively eliminate aziridine and re-form sextet Mn(II), **D**, in a spin-allowed step. This mechanism agrees well with the previously proposed mechanism [88].

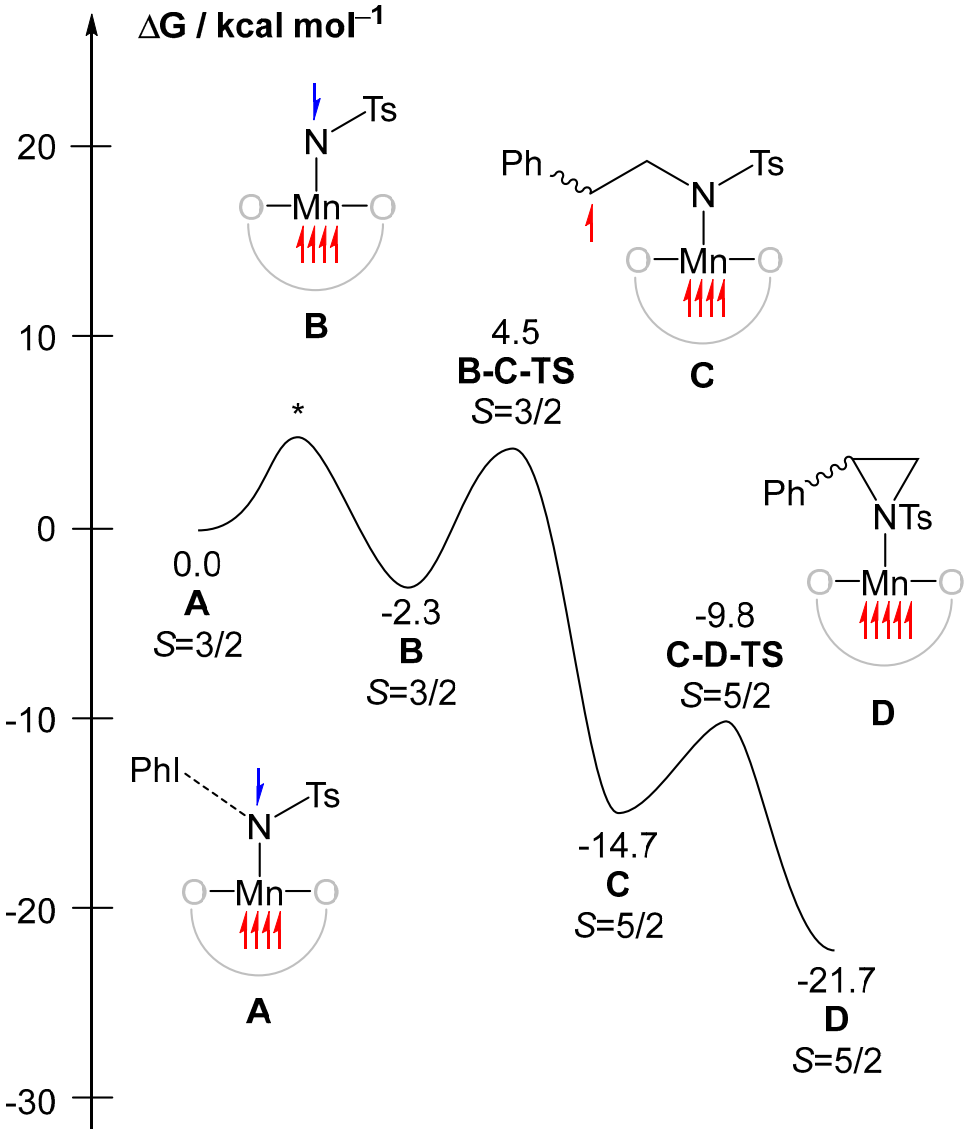

Figure 4. Reaction energy profile calculated at the B3LYP-D3(BJ)/def2-TZVP//BP86-D3(BJ)/def2-SVP level of theory. * indicates a missing transition state. Up and down spins are indicated by red and blue electrons, respectively.

The possible catalytic cycle (combining the spectroscopic and computational findings described above) is given in Scheme 2 below. The formation of PhINT adduct **A** is followed by the dissociation of PhI and facile formation of Mn(III)-imidyl radical **B** (free PhI is observed by NMR). While our computational studies focused on the reaction path in which PhINTs replace both THF ligands, it is possible that one THF remains coordinated to the metal throughout the reaction mechanism. Next, reactive (high-energy) species **B** reacts with styrene to form lower-energy radical intermediate **C**. As **C** is significantly more stable and the reaction barrier is low, little discrimination is observed between different para-substituted styrenes (featuring different electronic effects in the sterically remote para position). However, the reaction is anticipated to be sensitive to a more pronounced steric

effect, including styrene di-substitution. Likely due to the reactive radical nature of the reaction, complex mixtures of the reaction products were observed for the β-disubstituted styrenes. Subsequent C—N coupling forms azidine adduct **D**, which restores **A**, liberating the aziridine product.

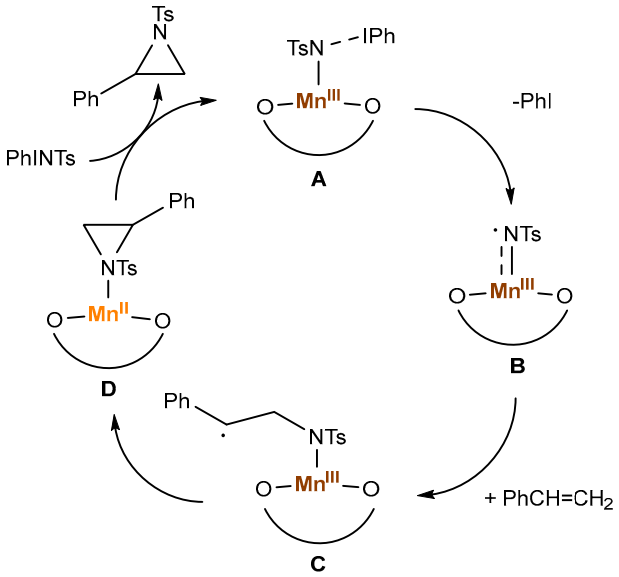

Scheme 2. Possible mechanism for styrene aziridination catalyzed by **2**.

3. Summary and Conclusions

We have reported the synthesis and aziridination reactivity of a new manganese complex Mn[O-terphenyl-O]^{Ph}(THF)$_2$, ligated by a bulky chelating bis(alkoxide) ligand. While the complex did not exhibit a reaction with an organoazide, its treatment with a mixture of PhINTs and styrene led to the formation of 2-phenyl-1-tosylaziridine in a good yield (up to 79%) with 10 mol% of the catalyst at room temperature. Various *p*-substituted styrenes, as well as the α-methyl-styrene produce the corresponding aziridines in comparable moderate yields; no reactivity with aliphatic olefins was observed. DFT calculations suggest a radical reaction intermediate, which is formed upon reaction of the high-spin imidyl radical Mn^{III}[O-terphenyl-O]^{Ph}(=NTs•) with styrene. Whereas the reactivity of the Mn bis(alkoxide) aziridination catalyst is not superior to the other known Mn aziridination catalysts (described in the Introduction), it (1) allows styrene aziridination relatively efficiently under sustainable (PhINTs:styrene 1:1 ratio) conditions, and (2) represents the first example of nitrene transfer into olefin by a 3d complex in a bulky bis(alkoxide) ligand environment. Our future studies will focus on the additional group-transfer reactions of middle and late 3d complexes in weak-field alkoxide ligand environments, and on the attempts to isolated and structurally and spectroscopically characterize various reaction intermediates.

4. Materials and Methods

4.1. General Methods and Characterization

Air-sensitive reactions were carried out in a nitrogen-filled glovebox. $MnCl_2$ and $KN(SiMe_3)_2$ were purchased from Strem chemicals and Sigma-Aldrich, respectively, and used as received. 2-bromophenylboronic acid, 1,4-diiodobenzene, and K_2CO_3 were purchased from Sigma-Aldrich and used as received. H_2[O-terphenyl-O]^{Ph} and PhINTs were synthesized based on the literature procedures [97,104]. Benzene-d_6 was purchased from Cambridge Isotope Laboratories and stored over 3 Å molecular sieves. HPLC-grade non-deuterated solvents were purchased from Sigma-Aldrich and purified using an MBraun solvent purification system. Compounds were generally characterized by ^{1}H and ^{13}C NMR, high-resolution mass spectrometry, and/or elemental analysis. Selected compounds were characterized by X-ray crystallography. NMR spectra were recorded at the Lumigen

Instrument Center on an Agilent 400 MHz Spectrometer and an Agilent DD2-600 MHz Spectrometer in C_6D_6 or $CDCl_3$ at room temperature. Chemical shifts and coupling constants (*J*) were reported in parts per million and Hertz, respectively. The solution state effective magnetic moment of **2** was determined using the Evans method. Elemental analysis was carried out by Midwest Microlab LLC under air-free conditions. A Thermo Fisher Scientific LTQ Orbittrap XL mass spectrometer at the Lumigen Instrument Centre was used for high-resolution mass spectra. IR spectra of powdered samples were recorded on a Shimadzu IR Affinity-1 FT-IR Spectrometer outfitted with an MIRacle10 attenuated total reflectance accessory with a monolithic diamond crystal stage and pressure clamp. UV-visible spectra were obtained using a Shimadzu UV-1800 spectrometer. GC-MS analysis was carried out using an Agilent 6890N spectrometer, Thermo TG5MS 30 m × 0.32 mm × 0.25 µm column, 7683 series injector, and Agilent 5973 detector.

*4.2. Synthesis of Mn[O-terphenyl-O]^{Ph}(THF)$_2$ (**2**)*

A 57 mg solution of ligand (0.096 mmol, 1 eq.) in THF was added dropwise to a 5 mL THF solution of $Mn[N(SiMe_3)_2]_2(THF)_2$ [105] (0.050 g, 0.096 mmol, 1 eq.). The color of the reaction changed from purple to light brown over the course of 12 h. The volatiles were removed under vacuum, and the crude product was recrystallized using a DCM-THF solvent mixture at −35 °C to give the complex 88% yield (0.061 mg, 0.077 mmol). IR (cm^{-1}, selected peaks) 2942 (m), 2899 (m), 2366 (m), 1490 (s), 1439 (s), 1115 (s), 1173 (s), 1073 (s), 1026 (s), 909 (s), 888 (s), 832 (s), 790 (s), 755 (s), 700 (s), and 638 (s). The UV−vis spectrum was nearly featureless in the 350–800 nm region (Figure S5). The magnetic moment for the compound was determined using the Evans method; two measurements (Figures S1 and S2) yielded μ_{eff} values of 5.68 and 5.97 μ_B. Anal. Calc for $C_{52}H_{46}MnO_4$: C, 79.07; H, 5.87. Found: C, 79.84; H, 6.21.

4.3. General Procedure for Catalytic Formation of Aziridines

A vial containing solid PhINTs (1 eq.) was transferred to a stirred C_6D_6 solution containing mesitylene (internal standard), alkene (1 eq.) and Mn[O-terphenyl-O]^{Ph}(THF)$_2$ (0.1 eq.). The color of the solution changed from colorless to brown. The NMR of the solution was collected after 24 h, and the yield was calculated with reference to the internal standard. Major products were identified by NMR and GC-MS. C_6D_6 was removed under vacuum, and the crude mixture was dissolved in $CDCl_3$. A comparison of the NMR with literature reports confirmed the formation of aziridines [106–108].

4.4. Computational Methods

Calculations were performed using density functional theory, as implemented in Gaussian 09 [109]. Geometry optimizations and frequency calculations [110], and wavefunction stability analyses [111] were executed at the BP86-D3(BJ)/def2-SVP level of theory employing density fitting and ultrafine grids [112–116]. Subsequent single-point energy refinements were performed at the B3LYP-D3(BJ)/def2-TZVP level of theory with ultrafine grids [114,117–120]. Structural analysis and orbital/spin density visualization were done in GaussView 06 [121]. Mayer bond orders were calculated using Multiwfn 3.5 [122].

Supplementary Materials: The following supporting information can be downloaded at https://www.mdpi.com/article/10.3390/molecules27185751/s1, ^{1}H NMR and GC-MS spectra of the aziridine products (Figures S14–S27), characterization data for complex **2** (Figures S1–S13), computational details, including energies, frequencies, and optimized geometries, for all species (Figures S28–S30, Tables S1–S3), crystal and refinement data for **2** (Table S4). CCDC 2183156.

Author Contributions: S.G. and S.S.K. designed and carried out the synthetic part of this work; N.M.W. and R.L.L. designed and carried out the computational part of this work; all authors participated in manuscript preparation. All authors have read and agreed to the published version of the manuscript.

Funding: This research was funded by the National Science Foundation, Division of Chemistry, grant number CHE 1855681. R.L.L. additionally acknowledges NSF for computational resources through MRI CHE-1919571.

Institutional Review Board Statement: Not applicable.

Informed Consent Statement: Not applicable.

Data Availability Statement: Information about Supplementary material is provided above in "Supplementary Materials" statement.

Acknowledgments: Experimental characterization was carried out at the Lumigen Instrument Center of Wayne State University.

Conflicts of Interest: The authors declare no conflict of interest.

References

1. Sweeney, J.B. Aziridines: Epoxides' Ugly Cousins? *Chem. Soc. Rev.* **2002**, *31*, 247–258. [PubMed]
2. Paike, V.V.; Kauthale, S.S.; Kumar, R.C.; Katariya, M.V.; More, R.R.; Ameta, K.L.; Mane, S.B. Aziridines: Synthesis and bioactivity. In *Bioactive Heterocycles*; Ameta, K.L., Pawar, R.P., Domb, A.J., Eds.; Nova Scientific Publishers: Hauppauge, NY, USA, 2013; pp. 41–68.
3. Kametani, T.; Honda, T. Application of Aziridines to the Synthesis of Natural Products. *Adv. Heterocycl. Chem.* **1986**, *39*, 181–236.
4. Werner, L.; Machara, A.; Sullivan, B.; Carrera, I.; Moser, M.; Adams, D.R.; Hudlicky, T. Several Generations of Chemoenzymatic Synthesis of Oseltamivir (Tamiflu): Evolution of Strategy, Quest for a Process-Quality Synthesis, and Evaluation of Efficiency Metrics. *J. Org. Chem.* **2011**, *76*, 10050–10067.
5. Hanessian, S.; Guesne, S.; Chenard, E. Total Synthesis of "Aliskiren": The First Renin Inhibitor in Clinical Practice for Hypertension. *Org. Lett.* **2010**, *12*, 1816–1819. [PubMed]
6. Nikitjuka, A.; Jirgensons, A. Synthesis, Chemical And Biological Properties Of Aziridine-1-Carbaldehyde Oximes. *Chem. Heterocycl. Compd.* **2014**, *49*, 1669–1684.
7. Kinoshita, S.; Uzu, K.; Nakano, K.; Shimizu, M.; Takahashi, T.; Matsui, M. Mitomycin Derivatives. Preparation of Mitosane and Mitosene Compounds and Their Biological Activities. *J. Med. Chem.* **1971**, *14*, 103–109. [CrossRef] [PubMed]
8. Xie, Y.; Lu, C.; Zhao, B.; Wang, Q.; Yao, Y. Cycloaddition of Aziridine with CO_2/CS_2 Catalyzed by Amidato Divalent Lanthanide Complexes. *J. Org. Chem.* **2019**, *84*, 1951–1958.
9. Zhu, C.; Feng, J.; Zhang, J. Rhodium-catalyzed intermolecular [3+3] cycloaddition of vinyl aziridines with C,N-cyclic azomethine imines: Stereospecific Synthesis Of Chiral fused tricyclic 1,2,4-hexahydrotriazines. *Chem. Commun.* **2017**, *53*, 4688–4691.
10. Degennaro, L.; Trinchera, P.; Luisi, R. Recent Advances in the Stereoselective Synthesis of Aziridines. *Chem. Rev.* **2014**, *114*, 7881–7929.
11. Zhu, Y.; Wang, Q.; Cornwall, R.G.; Shi, Y. Organocatalytic Asymmetric Epoxidation and Aziridination of Olefins and Their Synthetic Applications. *Chem. Rev.* **2014**, *114*, 8199–8256.
12. Wenker, H. The Preparation of Ethylene Imine from Monoethanolamine. *J. Am. Chem. Soc.* **1935**, *57*, 2328. [CrossRef]
13. Marsini, M.A.; Reeves, J.T.; Desrosiers, J.N.; Herbage, M.A.; Savoie, J.; Li, Z.; Fandrick, K.R.; Sader, C.A.; McKibben, B.; Gao, D.A.; et al. Diastereoselective Synthesis of α-Quaternary Aziridine-2-Carboxylates via Aza-Corey-Chaykovsky Aziridination of N-Tert-Butanesulfinyl Ketimino Esters. *Org. Lett.* **2015**, *17*, 5614–5617. [CrossRef] [PubMed]
14. Dokli, I.; Matanovic, I.; Hamersak, Z. Sulfur ylide promoted synthesis of N-protected aziridines: A combined experimental and computational approach. *Chem. Eur. J.* **2010**, *16*, 11744–11752. [CrossRef] [PubMed]
15. Chang, J.W.W.; Ton, T.M.U.; Chan, P.W.H. Transition-Metal-Catalyzed Aminations and Aziridinations of C-H and C=C Bonds with Iminoiodinanes. *Chem. Rec.* **2011**, *11*, 331–357. [PubMed]
16. Darses, B.; Rodrigues, R.; Neuville, L.; Mazurais, M.; Dauban, P. Transition metal-catalyzed iodine(III)-mediated nitrene transfer reactions: Efficient tools for challenging syntheses. *Chem. Commun.* **2017**, *53*, 493–508.
17. Zhdankin, V.V.; Protasiewicz, J.D. Development of New Hypervalent Iodine Reagents with Improved Properties and Reactivity by Redirecting Secondary Bonds at Iodine Center. *Coord. Chem. Rev.* **2014**, *275*, 54–62. [CrossRef]
18. Karila, D.; Dodd, R.H. Recent Progress in Iminoiodane-Mediated Aziridination of Olefins. *Curr. Org. Chem.* **2011**, *15*, 1507–1538.
19. Uchida, T.; Katsuki, T. Asymmetric Nitrene Transfer Reactions: Sulfimidation, Aziridination and C-H Amination Using Azide Compounds as Nitrene Precursors. *Chem. Rec.* **2014**, *14*, 117–129.
20. Aujla, P.S.; Baird, C.P.; Taylor, P.C.; Mauger, H.; Vallée, Y. Can chloramine-T be a nitrene transfer agent? *Tetrahedron Lett.* **1997**, *38*, 7453–7456.
21. Cano, I.; Nicasio, M.C.; Pérez, P.J. Nitrene transfer reactions catalysed by copper(I) complexes in ionic liquid using chloramine-T. *Dalton Trans.* **2009**, *4*, 730–734. [CrossRef]
22. Antunes, A.M.M.; Marto, S.J.L.; Branco, P.S.; Prabhakar, S.; Lobo, A.M. Palladium(II)-promoted Aziridination of Olefins with Bromamine T as the Nitrogen Transfer Reagent. *Chem. Commun.* **2001**, *5*, 405–406.

23. Elkoush, T.; Mak, C.L.; Paley, D.W.; Campbell, M.G. Silver(II) and Silver(III) Intermediates in Alkene Aziridination with a Dinuclear Silver(I) Nitrene Transfer Catalyst. *ACS Catal.* **2020**, *10*, 4820–4826.
24. Mat Lani, A.S.; Schomaker, J.M. Site-Selective, Catalyst-Controlled Alkene Aziridination. *Synthesis* **2018**, *50*, 4462–4470.
25. Ju, M.; Weatherly, C.D.; Guzei, I.A.; Schomaker, J.M. Chemo- and Enantioselective Intramolecular Silver-Catalyzed Aziridinations. *Angew. Chem. Int. Ed.* **2017**, *56*, 9944–9948. [CrossRef] [PubMed]
26. Weatherly, C.; Alderson, J.M.; Berry, J.F.; Hein, J.E.; Schomaker, J.M. Catalyst-controlled nitrene transfer by tuning metal:ligand ratios: Insight into the mechanisms of chemoselectivity. *Organometallics* **2017**, *36*, 1649–1661. [CrossRef]
27. Safin, D.A.; Pialat, A.; Korobkov, I.; Murugesu, M. Unprecedented Trinuclear AgI Complex with 2,4,6-Tris (2-pyrimidyl)-1,3,5-triazine as an Efficient Catalyst for the Aziridination of Olefins. *Chem. Eur. J.* **2015**, *21*, 6144–6149. [CrossRef]
28. Maestre, L.; Sameera, W.M.C.; Diaz-Requejo, M.M.; Maseras, F.; Perez, P.J. A General Mechanism for the Copper- and Silver-Catalyzed Olefin Aziridination Reactions: Concomitant Involvement of the Singlet and Triplet Pathways. *J. Am. Chem. Soc.* **2013**, *135*, 1338–1348.
29. Lee, S.; Jang, Y.J.; Phipps, E.J.T.; Lei, H.; Rovis, T. Rhodium(III)-Catalyzed Three-Component 1,2-Diamination of Unactivated Terminal Alkenes. *Synthesis* **2020**, *52*, 1247–1252. [CrossRef]
30. Azek, E.; Spitz, C.; Ernzerhof, M.; Lebel, H. A Mechanistic Study of the Stereochemical Outcomes of Rhodium-Catalysed Styrene Aziridinations. *Adv. Syn. Catal.* **2020**, *362*, 384–397.
31. Lee, S.; Lei, H.; Rovis, T. A Rh(III)-Catalyzed Formal [4+1] Approach to Pyrrolidines from Unactivated Terminal Alkenes and Nitrene Sources. *J. Am. Chem. Soc.* **2019**, *141*, 12536–12540. [CrossRef]
32. Sabir, S.; Pandey, C.B.; Yadav, A.K.; Tiwari, B.; Jat, J.L. Direct N-H/N-Me Aziridination of Unactivated Olefins Using O-(Sulfonyl)hydroxylamines as Aminating Agents. *J. Org. Chem.* **2018**, *83*, 12255–12260. [PubMed]
33. Su, J.Y.; Olson, D.E.; Ting, S.I.; Du Bois, J. Synthetic Studies Toward Pactamycin Highlighting Oxidative C-H and Alkene Amination Technologies. *J. Org. Chem.* **2018**, *83*, 7121–7134.
34. Ciesielski, J.; Dequirez, G.; Retailleau, P.; Gandon, V.; Dauban, P. Rhodium-Catalyzed Alkene Difunctionalization with Nitrenes. *Chem. Eur. J.* **2016**, *22*, 9338–9347. [PubMed]
35. Olson, D.E.; Su, J.Y.; Roberts, D.A.; Du Bois, J. Vicinal Diamination of Alkenes under Rh-Catalysis. *J. Am. Chem. Soc.* **2014**, *136*, 13506–13509.
36. Smith, D.T.; Njardarson, J.T. A scalable rhodium-catalyzed intermolecular aziridination reaction. *Angew. Chem. Int. Ed.* **2014**, *53*, 4278–4280.
37. Jat, J.L.; Paudyal, M.P.; Gao, H.; Xu, Q.-L.; Yousufuddin, M.; Devarajan, D.; Ess, D.H.; Kurti, L.; Falck, J.R. Direct Stereospecific Synthesis of Unprotected N-H and N-Me Aziridines from Olefins. *Science* **2014**, *343*, 61–65. [PubMed]
38. Wu, K.; Zhou, C.-Y.; Che, C.-M. Perfluoroalkyl Aziridines with Ruthenium Porphyrin Carbene Intermediates. *Org. Lett.* **2019**, *21*, 85–89.
39. Sengupta, G.; Pandey, P.; De, S.; Ramapanicker, R.; Bera, J.K. A bromo-capped diruthenium(II) N-heterocyclic carbene compound for in situ bromine generation with NBS: Catalytic olefin aziridination reactions. *Dalton Trans.* **2018**, *47*, 11917–11924.
40. Kim, C.; Uchida, T.; Katsuki, T. Asymmetric olefin aziridination using a newly designed Ru(CO)(salen) complex as the catalyst. *Chem. Commun.* **2012**, *48*, 7188–7190.
41. Tso, K.C.-H.; Chan, S.L.-F.; Huang, J.-S.; Che, C.-M. Wheel-to-rhomboid isomerization as well as nitrene transfer catalysis of ruthenium-thiolate wheels. *Chem. Commun.* **2017**, *53*, 2419–2422.
42. Rossi, S.; Puglisi, A.; Benaglia, M.; Carminati, D.M.; Intrieri, D.; Gallo, E. Synthesis in mesoreactors: Ru(porphyrin)CO-catalyzed aziridination of olefins under continuous flow conditions. *Catal. Sci. Technol.* **2016**, *6*, 4700–4704. [CrossRef]
43. Zardi, P.; Pozzoli, A.; Ferretti, F.; Manca, G.; Mealli, C.; Gallo, E. A mechanistic investigation of the ruthenium porphyrin catalyzed aziridination of olefins by aryl azides. *Dalton Trans.* **2015**, *44*, 10479–10489. [CrossRef] [PubMed]
44. Law, S.-M.; Chen, D.; Chan, S.L.-F.; Guan, X.; Tsui, W.-M.; Huang, J.-S.; Zhu, N.; Che, C.-M. Ruthenium Porphyrins with Axial π-Conjugated Arylamide and Arylimide Ligands. *Chem. Eur. J.* **2014**, *20*, 11035–11047. [CrossRef] [PubMed]
45. Zhang, J. Origins of the enantioselectivity of a palladium catalyst with BINOL-phosphoric acid ligands. *Org. Biomol. Chem.* **2018**, *16*, 8064–8071. [CrossRef]
46. Smalley, A.P.; Gaunt, M.J. Mechanistic Insights into the Palladium-Catalyzed Aziridination of Aliphatic Amines by C-H Activation. *J. Am. Chem. Soc.* **2015**, *137*, 10632–10641. [CrossRef]
47. Han, J.; Li, Y.; Zhi, S.; Pan, Y.; Timmons, C.; Li, G. Palladium-catalyzed aziridination of alkenes using N,N-dichloro-p-toluenesulfonamide as nitrogen source. *Tetrahedron Lett.* **2006**, *47*, 7225–7228. [CrossRef]
48. Fingerhut, A.; Serdyuk, O.V.; Tsogoeva, S.B. Non-heme iron catalysts for epoxidation and aziridination reactions of challenging terminal alkenes: Towards sustainability. *Green Chem.* **2015**, *17*, 2042–2058. [CrossRef]
49. Jenkins, D.M. Atom-economical C2 + N1 aziridination: Progress towards catalytic intermolecular reactions using alkenes and aryl azides. *Synlett* **2012**, *23*, 1267–1270. [CrossRef]
50. Breslow, R.; Gellman, S.H. Tosylamidation of Cyclohexane by a Cytochrome P-450 Model. *J. Chem. Soc. Chem. Commun.* **1982**, *24*, 1400–1401. [CrossRef]
51. Coin, G.; Patra, R.; Rana, S.; Biswas, J.P.; Dubourdeaux, P.; Clemancey, M.; de Visser, S.P.; Maiti, D.; Maldivi, P.; Latour, J.-M. Fe-Catalyzed Aziridination Is Governed by the Electron Affinity of the Active Imido-Iron Species. *ACS Catal.* **2020**, *10*, 10010–10020. [CrossRef]

52. Du, Y.-D.; Zhou, C.-Y.; To, W.-P.; Wang, H.-X.; Che, C.-M. Iron porphyrin catalysed light driven C-H bond amination and alkene aziridination with organic azides. *Chem. Sci.* **2020**, *11*, 4680–4686. [CrossRef] [PubMed]
53. Damiano, C.; Gadolini, S.; Intrieri, D.; Lay, L.; Colombo, C.; Gallo, E. Iron and Ruthenium Glycoporphyrins: Active Catalysts for the Synthesis of Cyclopropanes and Aziridines. *Eur. J. Inorg. Chem.* **2019**, *41*, 4412–4420. [CrossRef]
54. Shehata, M.F.; Ayer, S.K.; Roizen, J.L. Iron(MCP) Complexes Catalyze Aziridination with Olefins As Limiting Reagents. *J. Org. Chem.* **2018**, *83*, 5072–5081. [CrossRef] [PubMed]
55. Damiano, C.; Intrieri, D.; Gallo, E. Aziridination of Alkenes Promoted by Iron or Ruthenium Complexes. *Inorg. Chim. Acta* **2018**, *470*, 51–67. [CrossRef]
56. Hennessy, E.T.; Liu, R.Y.; Iovan, D.A.; Duncan, R.A.; Betley, T.A. Iron-mediated intermolecular N-group transfer chemistry with olefinic substrates. *Chem. Sci.* **2014**, *5*, 1526–1532. [CrossRef]
57. Liang, L.; Lv, H.; Yu, Y.; Wang, P.; Zhang, J.-L. Iron(III) Tetrakis(pentafluorophenyl)Porpholactone Catalyzes Nitrogen Atom Transfer to C:C and C-H Bonds with Organic Azides. *Dalton Trans.* **2012**, *41*, 1457–1460. [CrossRef]
58. Iovan, D.A.; Betley, T.A. Characterization of Iron-Imido Species Relevant for N-Group Transfer Chemistry. *J. Am. Chem. Soc.* **2016**, *138*, 1983–1993. [CrossRef]
59. Liu, Y.; Che, C.-M. [FeIII(F20-tpp)Cl] Is an Effective Catalyst for Nitrene Transfer Reactions and Amination of Saturated Hydrocarbons with Sulfonyl and Aryl Azides as Nitrogen Source under Thermal and Microwave-Assisted Conditions. *Chem. Eur. J.* **2010**, *16*, 10494–10501. [CrossRef]
60. Klotz, K.L.; Slominski, L.M.; Riemer, M.E.; Phillips, J.A.; Halfen, J.A. Mechanism of the Iron-Mediated Alkene Aziridination Reaction: Experimental and Computational Investigations. *Inorg. Chem.* **2009**, *48*, 801–803. [CrossRef]
61. Heins, S.P.; Morris, W.D.; Wolczanski, P.T.; Lobkovsky, E.B.; Cundari, T.R. Nitrene Insertion into C-C and C-H Bonds of Diamide Diimine Ligands Ligated to Chromium and Iron. *Angew. Chem. Int. Ed.* **2015**, *54*, 14407–14411. [CrossRef]
62. van Leest, N.P.; Tepaske, M.A.; Venderbosch, B.; Oudsen, J.-P.H.; Tromp, M.; van der Vlugt, J.I.; de Bruin, B. Electronically Asynchronous Transition States for C–N Bond Formation by Electrophilic [CoIII(TAML)]-Nitrene Radical Complexes Involving Substrate-to-Ligand Single-Electron Transfer and a Cobalt-Centered Spin Shuttle. *ACS Catal.* **2020**, *10*, 7449–7463. [CrossRef] [PubMed]
63. Hu, Y.; Lang, K.; Tao, J.; Marshall, M.K.; Cheng, Q.; Cui, X.; Wojtas, L.; Zhang, X.P. Next-Generation D2-Symmetric Chiral Porphyrins for Cobalt(II)-Based Metalloradical Catalysis: Catalyst Engineering by Distal Bridging. *Angew. Chem. Int. Ed.* **2019**, *58*, 2670–2674. [CrossRef] [PubMed]
64. Jiang, H.; Lang, K.; Lu, H.; Wojtas, L.; Zhang, X.P.J. Asymmetric Radical Bicyclization of Allyl Azidoformates via Cobalt(II)-Based Metalloradical Catalysis. *J. Am. Chem. Soc.* **2017**, *139*, 9164–9167. [CrossRef] [PubMed]
65. Lu, H.; Jiang, H.; Hu, Y.; Wojtas, L.; Zhang, X.P. Chemoselective intramolecular allylic C-H amination versus C:C aziridination through Co(II)-based metalloradical catalysis. *Chem. Sci.* **2011**, *2*, 2361–2366. [CrossRef]
66. Kalra, A.; Bagchi, V.; Paraskevopoulou, P.; Das, P.; Ai, L.; Sanakis, Y.; Raptopoulos, G.; Mohapatra, S. Choudhury, A.; Sun, Z.; et al. Is the Electrophilicity of the Metal Nitrene the Sole Predictor of Metal-Mediated Nitrene Transfer to Olefins? Secondary Contributing Factors as Revealed by a Library of High-Spin Co(II) Reagents. *Organometallics* **2021**, *40*, 1974–1996. [CrossRef]
67. Coin, G.; Patra, R.; Clemancey, M.; Dubourdeaux, P.; Pecaut, J.; Lebrun, C.; Castro, L.; Maldivi, P.; Chardon-Noblat, S.; Latour, J.-M. Fe-based Complexes as Styrene Aziridination Catalysts: Ligand Substitution Tunes Catalyst Activity. *ChemCatChem* **2019**, *11*, 5296–5299. [CrossRef]
68. Patra, R.; Coin, G.; Castro, L.; Dubourdeaux, P.; Clemancey, M.; Pecaut, J.; Lebrun, C.; Maldivi, P.; Latour, J.-M. Rational design of Fe catalysts for olefin aziridination through DFT-based mechanistic analysis. *Catal. Sci. Technol.* **2017**, *7*, 4388–4400. [CrossRef]
69. Blatchford, K.M.; Mize, C.J.; Roy, S.; Jenkins, D.M. Toward Asymmetric Aziridination with an Iron Complex Supported by a D2-symmetric Tetra-NHC. *Dalton Trans.* **2022**, *51*, 6153–6156. [CrossRef]
70. Isbill, S.B.; Chandrachud, P.P.; Kern, J.L.; Jenkins, D.M.; Roy, S. Elucidation of the Reaction Mechanism of C2 + N1 Aziridination from Tetracarbene Iron Catalysts. *ACS Catal.* **2019**, *9*, 6223–6233. [CrossRef]
71. Crandell, D.W.; Munoz, S.B.; Smith, J.M.; Baik, M.-H. Mechanistic study of styrene aziridination by iron(IV) nitrides. *Chem. Sci.* **2018**, *9*, 8542–8552. [CrossRef]
72. Chandrachud, P.P.; Bass, H.M.; Jenkins, D.M. Synthesis of Fully Aliphatic Aziridines with a Macrocyclic Tetracarbene Iron Catalyst. *Organometallics* **2016**, *35*, 1652–1657. [CrossRef]
73. Munoz, S.B., III; Lee, W.-T.; Dickie, D.A.; Scepaniak, J.J.; Subedi, D.; Pink, M.; Johnson, M.D.; Smith, J.M. Styrene Aziridination by Iron(IV) Nitrides. *Angew. Chem. Int. Ed.* **2015**, *54*, 10600–10603. [CrossRef] [PubMed]
74. Cramer, S.A.; Hernandez Sanchez, R.; Brakhage, D.F.; Jenkins, D.M. Probing the Role of an Fe(IV) Tetrazene in Catalytic Aziridination. *Chem. Commun.* **2014**, *50*, 13967–13970. [CrossRef] [PubMed]
75. Cramer, S.A.; Jenkins, D.M. Synthesis of Aziridines from Alkenes and Aryl Azides with a Reusable Macrocyclic Tetracarbene Iron Catalyst. *J. Am. Chem. Soc.* **2011**, *133*, 19342–19345. [CrossRef] [PubMed]
76. Wang, L.; Hu, L.; Zhang, H.; Chen, H.; Deng, L. Three-Coordinate Iron(IV) Bisimido Complexes with Aminocarbene Ligation: Synthesis, Structure, and Reactivity. *J. Am. Chem. Soc.* **2015**, *137*, 14196–14207. [CrossRef]
77. Liu, Q.; Long, L.; Ma, P.; Ma, Y.; Leng, X.; Xiao, J.; Chen, H.; Deng, L. Synthesis, Structure, and C–H Bond Activation Reaction of An Iron(IV) Terminal Imido Complex Bearing Trifluoromethyl Groups. *Cell. Rep. Phys. Sci.* **2021**, *2*, 100454. [CrossRef]

78. Abu-Omar, M.M. High-valent iron and manganese complexes of corrole and porphyrin in atom transfer and dioxygen evolving catalysis. *Dalton Trans.* **2011**, *40*, 3435–3444. [CrossRef]
79. Fantauzzi, S.; Caselli, A.; Gallo, E. Nitrene transfer reactions mediated by metallo-porphyrin complexes. *Dalton Trans.* **2009**, *28*, 5434–5443. [CrossRef]
80. Chinkov, N. Catalytic enantioselective reactions using organomanganese compounds. In *The Chemistry of Organomanganese Compounds*; Rappoport, Z., Marek, I., Eds.; John Wiley & Sons Ltd.: Chichester, UK, 2011.
81. Mansuy, D.; Mahy, J.P.; Dureault, A.; Bedi, G.; Battioni, P. Iron- and Manganese-Porphyrin Catalysed Aziridination of Alkenes by Tosyl- and Acyl-Iminoiodobenzene. *J. Chem. Soc. Chem. Commun.* **1984**, *17*, 1161–1163. [CrossRef]
82. Liang, J.-L.; Huang, J.-S.; Yu, X.-Q.; Zhu, N.; Che, C.-M. Metalloporphyrin-mediated asymmetric nitrogen-atom transfer to hydrocarbons: Aziridination of alkenes and amidation of saturated C-H bonds catalyzed by chiral ruthenium and manganese porphyrins. *Chem. Eur. J.* **2002**, *8*, 1563–1572. [CrossRef]
83. Noda, K.; Hosoya, N.; Irie, R.; Ito, Y.; Katsuki, T. Asymmetric Aziridination by Using Optically Active (Salen) Manganese(III) Complexes. *Synlett* **1993**, *7*, 469–471. [CrossRef]
84. O'Connor, K.J.; Wey, S.J.; Burrows, C. Alkene aziridination and epoxidation catalyzed by chiral metal salen complexes. *Tetrahedron Lett.* **1992**, *33*, 1001–1004. [CrossRef]
85. Zdilla, M.J.; Abu-Omar, M.M. Mechanism of Catalytic Aziridination with Manganese Corrole: The Often Postulated High-Valent Mn(V) Imido Is Not the Group Transfer Reagent. *J. Am. Chem. Soc.* **2006**, *128*, 16971–16979. [CrossRef] [PubMed]
86. Yan, S.Y.; Wang, Y.; Shu, Y.J.; Liu, H.H.; Zhou, X.G. Nitrene Transfer Reaction Catalyzed by Substituted Metallophthalocyanines. *J. Mol. Catal. A Chem.* **2006**, *248*, 148–151. [CrossRef]
87. Liang, S.; Jensen, M.P. Half-Sandwich Scorpionates as Nitrene Transfer Catalysts. *Organometallics* **2012**, *31*, 8055–8058. [CrossRef]
88. Bagchi, V.; Kalra, A.; Das, P.; Paraskevopoulou, P.; Gorla, S.; Ai, L.; Wang, Q.; Mohapatra, S.; Choudhury, A.; Sun, Z.; et al. Comparative Nitrene-Transfer Chemistry to Olefinic Substrates Mediated by a Library of Anionic Mn(II) Triphenylamido-Amine Reagents and M(II) Congeners (M = Fe, Co, Ni) Favoring Aromatic over Aliphatic Alkenes. *ACS Catal.* **2018**, *8*, 9183–9206. [CrossRef]
89. Grass, A.; Wannipurage, D.; Lord, R.L.; Groysman, S. Group-transfer chemistry at transition metal centers in bulky alkoxide ligand environments. *Coord. Chem. Rev.* **2019**, *400*, 1–16. [CrossRef]
90. Kurup, S.S.; Groysman, S. Catalytic Synthesis of Azoarenes via Metal-mediated Nitrene Coupling. *Dalton Trans.* **2022**, *51*, 4577–4589. [CrossRef]
91. Yousif, M.; Tjapkes, D.J.; Lord, R.L.; Groysman, S. Catalytic Formation of Asymmetric Carbodiimides at Mononuclear Chromium (II/IV) Bis(alkoxide) Complexes. *Organometallics* **2015**, *34*, 5119–5128. [CrossRef]
92. Yousif, M.; Wannipurage, D.; Huizenga, C.D.; Washnock-Schmid, E.; Peraino, N.J.; Ozarowski, A.; Stoian, S.A.; Lord, R.L.; Groysman, S. Catalytic Nitrene Homocoupling by an Iron(II) Bis(alkoxide) Complex: Bulking Up the Alkoxide Enables a Wider Range of Substrates and Provides Insight into the Reaction Mechanism. *Inorg. Chem.* **2018**, *57*, 9425–9438. [CrossRef]
93. Bellow, J.A.; Yousif, M.; Cabelof, A.C.; Lord, R.L.; Groysman, S. Reactivity Modes of an Iron Bis(alkoxide) Complex with Aryl Azides: Catalytic Nitrene Coupling vs Formation of Iron(III) Imido Dimers. *Organometallics* **2015**, *34*, 2917–2923. [CrossRef]
94. Wannipurage, D.; Kurup, S.S.; Groysman, S. Heterocoupling of Different Aryl Nitrenes to Produce Asymmetric Azoarenes Using Iron-Alkoxide Catalysis and Investigation of the Cis-Trans Isomerism of Selected Bulky Asymmetric Azoarenes. *Organometallics* **2021**, *40*, 3637–3644. [CrossRef]
95. Grass, A.; Dewey, N.S.; Lord, R.L.; Groysman, S. Ketenimine Formation Catalyzed by a High Valent Cobalt Carbene in Bulky Alkoxide Ligand Environment. *Organometallics* **2019**, *38*, 962–972. [CrossRef]
96. Grass, A.; Bellow, J.A.; Morrison, G.; zur Loye, H.-C.; Lord, R.L.; Groysman, S. One electron reduction transforms high-valent low-spin cobalt alkylidene into high-spin cobalt(II) carbene radical. *Chem. Commun.* **2020**, *56*, 8416–8419. [CrossRef] [PubMed]
97. Kurup, S.S.; Wannipurage, D.; Lord, R.L.; Groysman, S. An iron complex with a new chelating bis(alkoxide) ligand leads to an active nitrene dimerization catalyst for a variety of para- and meta-substituted azide precursors. *Chem. Commun.* **2019**, *55*, 10780–10783. [CrossRef]
98. Kurup, S.S.; Staples, R.J.; Lord, R.L.; Groysman, S. Synthesis of Chromium(II) Complexes with Chelating Bis(alkoxide) Ligand and Their Reactions with Organoazides and Diazoalkanes. *Molecules* **2020**, *25*, 373. [CrossRef]
99. Bellow, J.A.; Yousif, M.; Fang, D.; Kratz, E.G.; Cisneros, G.A.; Groysman, S. Synthesis and reactivity of 3d metal complexes with the bulky alkoxide ligand [OC^{t}Bu$_2$Ph]. *Inorg. Chem.* **2015**, *54*, 5624–5633. [CrossRef]
100. Bellow, J.A.; Martin, P.D.; Lord, R.L.; Groysman, S. Reductive Coupling of Azides Mediated by an Iron(II) Bis(alkoxide) Complex. *Inorg. Chem.* **2013**, *52*, 12335–12337. [CrossRef]
101. Eikey, R.A.; Khan, S.I.; Abu-Omar, M.M. The Elusive Terminal Imido of Manganese(V). *Angew. Chem. Int. Ed.* **2002**, *41*, 3591–3595. [CrossRef]
102. Lansky, D.E.; Kosack, J.R.; Narducci Sarjeant, A.A.; Goldberg, D.P. An Isolable, Nonreducible High-Valent Manganese(V) Imido Corrolazine Complex. *Inorg. Chem.* **2006**, *45*, 8477–8479. [CrossRef]
103. Shi, H.; Xie, J.; Lam, W.W.Y.; Man, W.-L.; Mak, C.-K.; Yiu, S.-M.; Lee, H.K.; Lau, T.-C. Generation and Reactivity of a One-Electron-Oxidized Manganese(V) Imido Complex with a Tetraamido Macrocyclic Ligand. *Chem. Eur. J.* **2019**, *25*, 12895–12899. [CrossRef]

104. Yamada, Y.; Yamamoto, T.; Okawara, M. Synthesis and Reaction of New Type I–N Ylide, N-Tosyliminoiodinane. *Chem. Lett.* **1975**, *4*, 361–362. [CrossRef]
105. Bradley, D.C.; Hursthouse, M.B.; Ibrahim, A.A.; Malik, K.M.A.; Motevalli, M.; Möseler, R.; Powell, H.; Runnacles, J.D.; Sullivan, A.C. Synthesis and chemistry of the bis(trimethylsilyl)amido bis-tetrahydrofuranates of the group 2 metals magnesium, calcium, strontium and barium. X-ray crystal structures of Mg[N(SiMe3)2]2·2THF and related Mn[N(SiMe3)2]2·2THF. *Polyhedron* **1990**, *9*, 2959–2964. [CrossRef]
106. Johnson, S.L.; Hilinski, M.K. Organocatalytic Olefin Aziridination via Iminium-Catalyzed Nitrene Transfer: Scope, Limitations, and Mechanistic Insight. *J. Org. Chem.* **2019**, *84*, 8589–8595. [CrossRef]
107. Minakata, S.; Morino, Y.; Oderaotoshia, Y.; Komatsu, M. Novel aziridination of olefins: Direct synthesis from sulfonamides using t-BuOI. *Chem. Commun.* **2006**, *31*, 3337–3339. [CrossRef]
108. Evans, D.A.; Faul, M.M.; Bilodeau, M.T. Development of the Copper-Catalyzed Olefin Aziridination Reaction. *J. Am. Chem. Soc.* **1994**, *116*, 2742–2753. [CrossRef]
109. Frisch, M.J.; Trucks, G.W.; Schlegel, H.B.; Scuseria, G.E.; Robb, M.A.; Cheeseman, J.R.; Scalmani, G.; Barone, V.; Mennucci, B.; Petersson, G.A.; et al. *Gaussian 09*; Revision D.01; Gaussian, Inc.: Wallingford, CT, USA, 2013.
110. Schlegel, H.B. Geometry optimization. *WIREs Comput. Mol. Sci.* **2011**, *1*, 790–809. [CrossRef]
111. Bauernschmitt, R.; Ahlrichs, R. Stability analysis for solutions of the closed shell Kohn-Sham equation. *J. Chem. Phys.* **1996**, *104*, 9047–9052. [CrossRef]
112. Becke, A.D. Density-functional exchange-energy approximation with correct asymptotic-behavior. *Phys. Rev. A* **1988**, *38*, 3098–3100. [CrossRef]
113. Perdew, J.P. Density-functional approximation for the correlation energy of the inhomogeneous electron gas. *Phys. Rev. B* **1986**, *33*, 8822–8824. [CrossRef]
114. Weigend, F.; Ahlrichs, R. Balanced basis sets of split valence, triple zeta valence, and quadruple zeta valence quality for H to Rn: Design and assessment of accuracy. *Phys. Chem. Chem. Phys.* **2005**, *7*, 3297–3305. [CrossRef] [PubMed]
115. Weigend, F. Accurate Coloumb-fitting basis sets for H to Rn. *Phys. Chem. Chem. Phys.* **2006**, *8*, 1057–1065. [CrossRef] [PubMed]
116. Bootsma, A.N.; Wheeler, S.E. Popular Integration Grids Can Result in Large Errors in DFT-Computed Free Energies. *ChemRxiv* **2019**. [CrossRef]
117. Vosko, S.H.; Wilk, L.; Nusair, M. Accurate spin-dependent electron liquid correlation energies for local spin density calculations: A critical analysis. *Can. J. Phys.* **1980**, *58*, 1200–1211. [CrossRef]
118. Lee, C.; Yang, W.; Parr, R.G. Development of the Colle-Salvetti correlation-energy formula into a functional of the electron density. *Phys. Rev. B* **1988**, *37*, 785–789. [CrossRef] [PubMed]
119. Becke, A.D. Density-functional thermochemistry. III. The role of exact exchange. *J. Chem. Phys.* **1993**, *98*, 5648–5652. [CrossRef]
120. Stephens, P.J.; Devlin, F.J.; Chabalowski, C.F.; Frisch, M.J. *Ab Initio* Calculation of Vibrational Absorption and Circular Dichroism Spectra Using Density Functional Force Fields. *J. Phys. Chem.* **1994**, *98*, 11623–11627. [CrossRef]
121. Dennington, R.; Keith, T.A.; Millam, J.M. *GaussView*, 6th ed.; Semichem Inc.: Shawnee Mission, KS, USA, 2016.
122. Lu, T.; Chen, F. Multiwfn: A Multifunctional Wavefunction Analyzer. *J. Comp. Chem.* **2012**, *33*, 580–592. [CrossRef]